Picosecond Dynamics of the Photoreduction of 4,4′-Bipyridine by 1,4-Diazabicyclo[2.2.2]octane in Water

Laurent Boilet, Guy Buntinx, Christophe Lefumeux, and Olivier Poizat*

LASIR, CNRS, Centre d'Etudes et de Recherches Lasers et Applications, bât. C5, Université de Lille I, 59655 Villeneuve d'Ascq Cedex, France

Received: April 3, 2002; In Final Form: July 23, 2002

The photoreduction of 4,4′-bipyridine (44BPY) by 1,4-diazabicyclo[2.2.2]octane (DABCO) has been studied in water by picosecond transient absorption spectroscopy and time-resolved resonance Raman spectroscopy. The kinetics of formation of the anion radical $44BPY^{-\bullet}$ by electron transfer have been analyzed and compared with those obtained previously for the same reaction in acetonitrile. The $44BPY^{-\bullet}$ anion is linked via H-bonding to the surrounding water molecules immediately after its formation and undergoes proton transfer along the H-bond to reach an acid−base equilibrium of $pK_a \cong 15$. The nature of the ion pair produced initially in the electron-transfer reaction is discussed.

1. Introduction

4,4′-Bipyridine (44BPY) is easily reduced by aliphatic amines upon photoexcitation due to favorable free energy change values for electron transfer at both the lowest excited singlet (S_1) and triplet (T_1) states. The precursor excited states, S_1 $n\pi^*$[1−3] and T_1 $\pi\pi^*$,[4,5] and the transient reduced species, the anion radical $44BPY^{-\bullet}$[4,6] or the N-hydro radical $44BPYH^{\bullet}$[5,7−9], have been well characterized by electronic (transient absorption) and vibrational (time-resolved resonance Raman) spectroscopy. In addition, the electronic configuration and geometrical structure of these species have been determined by quantum chemical calculation.[10−12] The 44BPY molecule appears thus well-suited for performing an extensive spectroscopic investigation of the mechanism of phototransfer of electron.

Recently, the photoreduction of 44BPY by triethylamine (TEA) and 1,4-diazabicyclo[2.2.2]octane (DABCO) has been examined in acetonitrile from picosecond transient absorption and time-resolved resonance Raman measurements.[13] It was found that, in the case of DABCO, the reaction at the S_1 state is essentially unproductive but the reaction at the T_1 state leads efficiently to the free anion radical in a picosecond time scale via the formation of a contact ion pair (CIP). In the presence of TEA as electron donor, a fast intrapair proton-transfer competes with the dissociation of the CIP and yields the N-hydro radical $44BPYH^{\bullet}$, in agreement with the highly basic character of the $44BPY^{-\bullet}$ anion[14] and the strong acidity of the $TEA^{+\bullet}$ cation radical.[15,16] The vibrational properties of the anion radical involved in a CIP were characterized by a specific Raman spectrum clearly distinguishable from the free anion one. Interestingly, the analysis of these data demonstrated that, despite the fast intrapair proton jump arising in the case of TEA, the 44BPY anion radical implicated in a CIP is not bound to the amine cation via hydrogen bonding. It was concluded that the transfer of proton arises as soon as the anion and cation species are favorably oriented, that is, the process is governed by the dynamics of reorientation of the two partners within the pair after the transfer of electron.

We are now interested in examining how the reaction dynamics is modified in the presence of protic solvents. The possible formation of a hydrogen bond between the highly basic anion radical and the surrounding solvent molecules may change drastically the intrapair reactivity. In particular, fast protonation by the solvent can be expected. In this respect, this reaction may be well-suited for studying the dynamics of intermolecular proton transfer through hydrogen bonding. In this paper, we present an experimental investigation of the picosecond dynamics of photoreduction of 44BPY by DABCO in water by using transient absorption and time-resolved Raman spectroscopy. Water was chosen as protic solvent because it does not interfere in the photochemistry of 44BPY. Alcohols were not appropriate to this study because they are efficient hydrogen atom donors toward the 44BPY excited states.[1,2,5,9] On the other hand, in contrast to $TEA^{+\bullet}$, the cation radical of DABCO is not a proton donor because its rigid bridged structure is unfavorable to the loss of a proton. The system investigated here is thus the simplest one for obtaining unmixed information on the role of water in the process.

2. Experimental Section

4,4′-Bipyridine (44BPY) and 1,4-diazabicyclo[2.2.2]octane (DABCO) were purchased from Aldrich. 44BPY was sublimed at 80 °C in vacuo prior to each measurement, and DABCO was used as received. All measurements were performed on 10^{-3}−10^{-2} M aqueous solutions of 4,4′-bipyridine using distilled deionized water or deuterium oxide (99.9 atom % D, Interchim).

The subpicosecond transient absorption and picosecond Raman scattering experiments have been already described.[1−3] Briefly, they were carried out by using a 1 kHz Ti−sapphire laser system based upon a Coherent (MIRA 900D) oscillator and a BM Industries (ALPHA 1000) regenerative amplifier. This system was set in a femtosecond configuration for all of the absorption measurements. Tripling the initial 90 fs pulses at 800 nm (0.5 mm BBO crystal) provided the pump excitation at 266 nm. Its power was limited to 10−20 μJ per pulse (1.0−2.0 mJ/cm^2). A probe white light continuum pulse was generated at 800 nm in a CaF_2 plate. The probe pulse was delayed in time relative to the pump pulse using an optical delay line

* To whom correspondence should be addressed. Fax: +33-320434085. E-mail: poizat@univ-lille1.fr.

10.1021/jp020882j CCC: $22.00
Published on Web 09/27/2002

(Microcontrol model MT160-250PP driven by an ITL09 controller, precision ±1 μm). The overall time resolution (fwhm of the pump−probe intensity cross-correlation) is estimated to be about 300 fs from the two-photon (pump + probe) absorption signal in pure hexane. The time dispersion of the continuum light over the 300−700 nm region of analysis is about 0.8 ps. The transmitted light was analyzed by a CCD optical multichannel analyzer (Princeton Instrument LN/CCD-1340/400-EB detector + ST-138 controller). Samples were circulating in a flow cell with 2.5 mm optical path length. Data were accumulated over 3 min (∼180 000 pump−probe sequences).

For the Raman measurements, the laser source was set in a picosecond configuration. Pump pulses at 253 nm (∼15 μJ, 20 mJ/cm^2 per pulse) and probe pulses at 380 nm (∼5 μJ) were obtained by frequency tripling and doubling, respectively, the Ti−sapphire fundamental tuned at 760 nm. The pump−probe cross-correlation fwhm was ∼4 ps. Scattered light was collected at 90° to the incident excitation and sent through a Notch filter into a home-built multichannel spectrometer coupled to a CCD optical multichannel analyzer (Princeton Instrument LN/CCD-1100-PB-UV/AR detector + ST-138 controller). The flowing jet sampling technique was adopted (1 mm diameter jet). The wavenumber shift was calibrated using the Raman spectra of indene. Data collection times were 10−20 min. In all absorption and Raman measurements, the pump−probe polarization configuration was set at the magic angle.

3. Results

Before going into details about the photoreduction of 44BPY by DABCO, we studied the state of solvation of the ground-state reactants 44BPY and DABCO in aqueous solution prior to the excitation. Both molecules are proton acceptor (pK_a = 4.82[14] and 8.82,[17] respectively). Although they are present exclusively as the deprotonated form in the experimental conditions of our measurements (DABCO concentration ≥ 0.5 M, pH ≥ 11), they may undergo hydrogen bonding in water. In a previous work,[1] it was shown that the Raman active ring-breathing mode frequency in 44BPY is specifically sensitive to hydrogen bonding, with a peak maximum at 995 cm^{-1} for the "free" form in acetonitrile or hexane and 1004 cm^{-1} for the H-bonded form in ethanol. In the present study, a more comprehensive analysis of the 44BPY Raman frequencies in aprotic solvents (including acetonitrile, diethyl ether, *n*-hexane, chloroform, and acetone) and protic solvents (including methanol, ethanol, 1,1,1,3,3,3-hexafluoro-2-propanol, and water), indicated that four vibrations ascribed to the ring C−C stretching and in-plane distortion motions, 8a, 19a, 12 and 1,[10] are affected by the formation of hydrogen bonds. These vibrations were observed, respectively, at 1615 ± 1, 1507 ± 1, 996 ± 1, and 756 ± 1 cm^{-1} in aprotic media and at 1622 ± 2, 1514 ± 3, 1007 ± 3, and 764 ± 2 cm^{-1} in protic solvents. In binary protic/aprotic solvents, a juxtaposition of the two components was observed for each one of these modes, indicating that both the "free" and H-bonded species are present. In water, only the high-frequency component was present, implying that all of the 44BPY molecules are H-bonded. The same observation was made in aqueous solutions containing 1 M DABCO: hydrogen bonding to 44BPY is preserved despite the strong basicity of the solution (pH = 11.4). A similar analysis made for the amine DABCO revealed that one vibration around 970 cm^{-1}, assigned to a mode involving predominantly C−C stretching character,[18] is particularly sensitive to the protic character of the solvent. Its large shift from 963 cm^{-1} in acetonitrile to 982 cm^{-1} in water is indicative of H-bonding in the latter case.

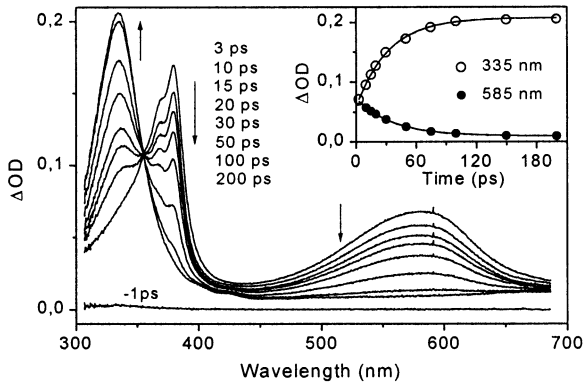

Figure 1. Transient absorption spectra of 44BPY (10^{-2} M) in H_2O at different delay times (0−200 ps) after 266 nm excitation. The inset shows the time dependence of the intensity measured at 335 and 585 nm.

A. Quenching by DABCO in H_2O. Transient absorption spectra of solutions of 44BPY and DABCO in water were recorded for five DABCO concentrations between 0.5 and 1.6 M at various times in the 0−1500 ps time range following subpicosecond excitation at 266 nm. This wavelength corresponds to the lowest energy $\pi\pi^*$ absorption band of 44BPY (ϵ_{266} = 7500 M^{-1} cm^{-1}). The absorption of DABCO at 266 nm is very weak. However, at the high concentrations used in the present study, it leads efficiently to the formation of the cation radical DABCO$^{+\bullet}$ and solvated electron by photoionization in water. At low 44BPY concentration (below 5 × 10^{-3} M), the photoionization of DABCO competes with the excitation of 44BPY and the observed spectral evolution was characteristic of the two processes, with superimposed kinetics. At high 44BPY concentration (10^{-2} M), excitation of DABCO was negligible and the evolution of the 44BPY chemical process was much easier to analyze. Measurements performed for different 44BPY concentrations in the range 5 × 10^{-4} to 10^{-2} M showed that the kinetics characterizing the 44BPY photoreduction reaction remain unchanged in all cases. They are thus unaffected by the presence, at low 44BPY concentration, of a simultaneous process of photoionization of DABCO, indicating that the solvated electron does not interfere with the 44BPY photochemistry in the 0−1500 ps time domain experienced in this study. They are also unaffected by the possible dimerization of 44BPY (aggregation effect) expected at high concentration. Accordingly, we present here the absorption measurements made with the highest 44BPY concentration (10^{-2} M), which are not obscured by the DABCO ionization process and can be analyzed more easily.

In the absence of DABCO (Figure 1), the time evolution of the spectra is characteristic of the intersystem crossing process (ISC) from the lowest excited S_1 state of 44BPY (382 and 590 nm bands) to the triplet state T_1 (339 nm band).[1] The decay of the S_1 state spectrum and the rise of the T_1 state band can be fit with the same single exponential kinetics (inset in Figure 1). Because ISC is the only significant decay process of S_1 in pure water (ϕ_{ISC} = 1),[1] the fit leads to a rate constant k_{ISC} of (2.8 ± 0.1) × 10^{10} s^{-1} (S_1 lifetime = 36 ps). The T_1 state is stable on this time scale (lifetime τ_0 = 70 μs[4]).

Figures 2 and 3 show the spectral evolution in the time domains 0−60 and 60−900 ps, respectively, of the transient absorption spectra obtained upon excitation of a solution of 44BPY (10^{-2} M) and DABCO (1.6 M) in water. We observe first, in the short time domain (Figure 2), a much faster decay of the S_1 state spectrum (about 15 ps) than that in pure water and a drastic reduction of the T_1 state yield. Both effects are

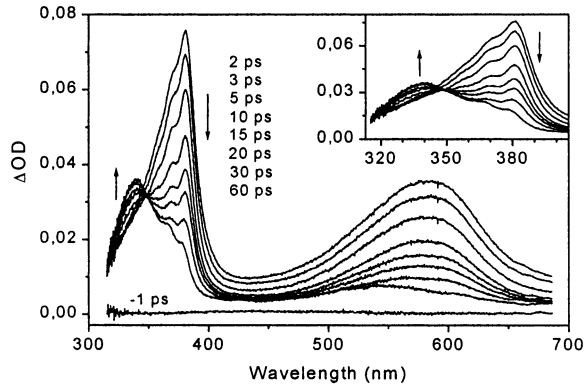

Figure 2. Transient absorption spectra of a solution of 44BPY (10^{-2} M) and DABCO (1.6 M) in H_2O at different delay times (0−60 ps) after 266 nm excitation. The inset shows an enlargement of the 310−405 nm region.

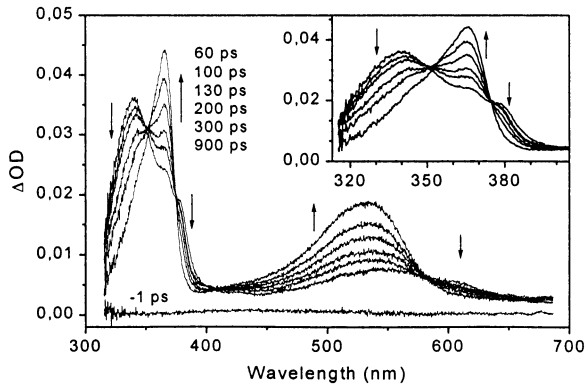

Figure 3. Transient absorption spectra of a solution of 44BPY (10^{-2} M) and DABCO (1.6 M) in H_2O at different delay times (60−900 ps) after 266 nm excitation. The inset shows an enlargement of the 310−405 nm region.

indicative of the fact that the S_1 state is quenched by DABCO. An isosbestic point is observed between the S_1 and T_1 spectra at 348 nm from 5 to 60 ps, but the shortest time spectra (2−5 ps range) are clearly outside this point. This anomaly is due to the effect of a band narrowing in the S_1 state spectrum in the first picoseconds, which is likely resulting from vibrational relaxation. Then (Figure 3), the T_1 state spectrum decays from 60 to 900 ps, and new bands appear simultaneously at 365 and 538 nm. These bands are unambiguously characterizing the N-hydro radical 44BPYH$^{\bullet}$.[5,8,9] An isosbestic point is apparent between the T_1 state and N-hydro radical spectra at 351 nm, which could suggest that a direct H-atom abstraction from DABCO arises on excitation. However, this hypothesis seems doubtful because the photolysis of 44BPY in acetonitrile in the presence of DABCO leads exclusively to an electron-transfer reaction.[13] On the other hand, we observe in Figure 3, in addition to the T_1 state and radical bands, the presence of two shoulders around 380 and 600 nm that decay together with the T_1 band but do not belong to the T_1 spectrum. These bands could correspond to the spectrum of the anion radical 44BPY$^{-\bullet}$. Three isosbestic points are noticed at 376, 409, and 583 nm between this new spectrum and N-hydro radical spectrum. No spectral evolution is discernible between 900 and 1500 ps.

To confirm the identification of the transient species involved in the reaction, time-resolved resonance Raman measurements were performed by using a probe excitation at 380 nm. According to the UV−visible absorption characteristics of these species, this wavelength appears in good resonance conditions for the S_1 state, anion radical, and N-hydro radical but almost

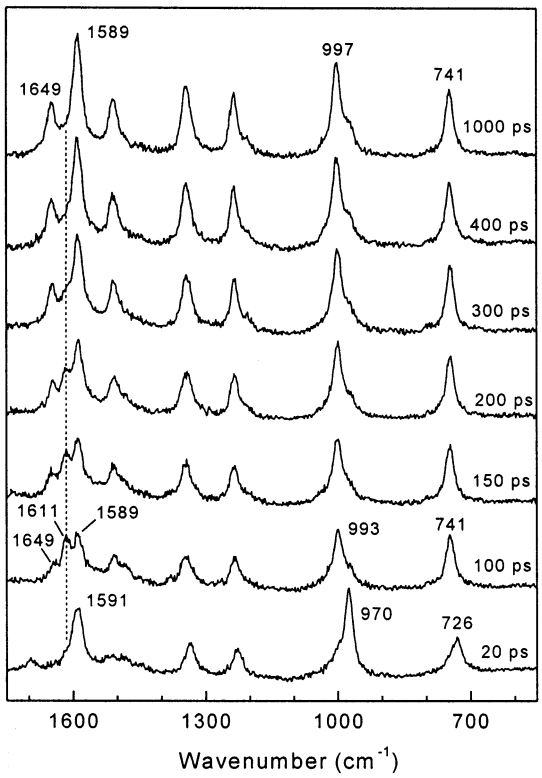

Figure 4. Time-resolved resonance Raman spectra of a solution of 44BPY (10^{-3} M) and DABCO (1 M) in H_2O probed at 380 nm at different delay times (20−1000 ps) after pump excitation at 253 nm. The probe-only spectrum (solvent and ground-state peaks) has been subtracted to all spectra. Some characteristic Raman frequencies are indicated. The dashed line points out the position of the 1611 cm^{-1} band typical of the anion radical 44BPY$^{-\bullet}$.

out of resonance for the T_1 state. Thus, this latter species cannot be observed in these conditions. Figure 4 shows the time evolution of the Raman spectra observed in the 20−1000 ps time range after excitation of a solution of 44BPY (10^{-3} M) and DABCO (1 M) in water. As expected, the 20 ps spectrum is characteristic of the S_1 state.[2,3] At 100 ps, the S_1 spectrum has completely disappeared (band at 726 cm^{-1}, for example) and new Raman bands are evolving with time up to about 1 ns. Two sets of Raman bands can be distinguished. One corresponds to the final spectrum of the kinetics (typical bands at 741, 997, 1589, and 1649 cm^{-1}) and increases with time from 50 ps to 1 ns. It is typical of the N-hydro radical 44BPYH$^{\bullet}$.[7] A second one is manifested at shorter times by the 1611 cm^{-1} band (indicated by a dashed line in Figure 4). Its intensity is negligible at 20 ps, increases with time up to about 100 ps, and then decreases concomitantly with the appearance of the radical spectrum. It becomes undetectable after 600 ps. A better characterization of this spectrum was obtained by subtracting the N-hydro radical contribution (1 ns spectrum) from the 100 ps spectrum. The residual spectrum is shown in Figure 5 (lower trace) together with the S_1 state (upper trace) and N-hydro radical (middle trace) spectra. It is obviously similar to the anion radical spectrum recorded at the same probe wavelength in acetonitrile[13] although some frequency shifts are noticed between the two solvents. This observation confirms definitely the transitory presence of 44BPY$^{-\bullet}$ during the reaction pathway. No frequency shifts were perceptible in the anion radical spectrum on going from 50 to 600 ps.

B. Kinetic Analysis. To examine quantitatively the mechanism of photoreduction of 44BPY by DABCO in water, we analyzed the experimental transient absorption spectra into three

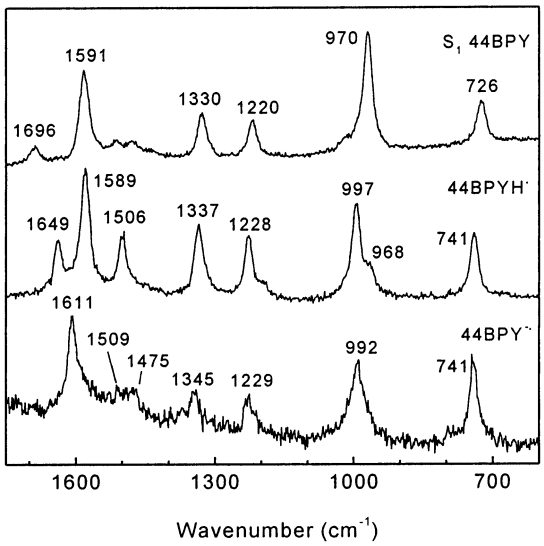

Figure 5. Comparison of the normalized Raman spectra of the 44BPY S_1 state (10 ps spectrum), 44BPYH$^{\bullet}$ radical (1 ns spectrum), and 44BPY$^{-\bullet}$ anion radical ([100 ps spectrum] − 0.25[1 ns spectrum]), obtained from the series of spectra displayed in Figure 4. The main band frequencies are indicated.

contributions. The first two ones were the T_1 state and N-hydro radical contributions, for which the 200 ps spectrum observed in the absence of DABCO (Figure 1) and the 900 ps spectrum observed in the presence of an excess of DABCO (1.6 M, Figure 3), respectively, were chosen as reference spectra. The third contribution was the residual spectrum obtained after subtraction of the above T_1 and N-hydro radical components. Below 60 ps, it corresponds to the sum of the S_1 state and anion radical contributions, which cannot be easily resolved because the two spectra are entirely overlapping (see Figure 2 in ref 13). Above 60 ps, it characterizes exclusively the anion radical species, 44BPY$^{-\bullet}$. The spectrum obtained in this way for the anion radical remains unchanged at all times in the 60−600 ps domain. It presents a sharp line at 378 nm and a broad band with maxima around 530, 562, and 604 nm. The kinetics characterizing the three above spectral contributions were plotted at the band maxima 339, 365, and 381 nm, respectively. The kinetic data corresponding to the series of absorption measurements shown in Figures 2 and 3 (1.6 M DABCO solution) are displayed in Figure 6, together with the best fit calculated according to a reaction model schematized by Scheme 1. This model assumes a sequential electron-transfer−proton-transfer reaction: the anion radical formed by electron-transfer quenching of the excited 44BPY is then protonated by the surrounding water solvent (tests to fit the experimental data with a model based on a parallel formation of the anion and N-hydro radical products were unsuccessful). The kinetic parameters describing the time evolution of the four transient species involved in this reaction scheme, that is, the S_1 and T_1 states, the anion radical, and the N-hydro radical, were determined to reproduce the three experimental kinetic contributions mentioned above for the five different DABCO concentrations investigated in this study.

The model incorporates quenching reactions of both the S_1 and T_1 states by DABCO. The triplet-state decay kinetics is monoexponential with a rate constant k^3 increasing linearly with the DABCO concentration, as expected for diffusional electron-transfer quenching (pseudo-first-order kinetics, $k^3 = (\tau_0^3)^{-1} + k_q^3$[DABCO], where τ_0^3 is the T_1 state lifetime in the absence of electron-donor quencher). A Stern−Volmer analysis provides a quenching rate constant of $k_q^3 = (4.8 \pm 0.3) \times 10^9$ M^{-1} s^{-1}.

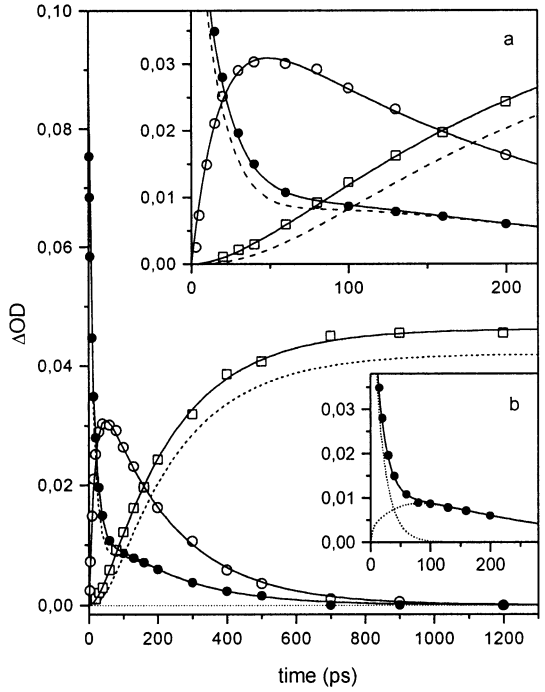

Figure 6. Time dependence of the extracted contributions of the T_1 state absorption at 339 nm (○) and N-hydro radical absorption at 365 nm (□) and of the residual absorption (S_1 state + anion radical) at 381 nm (●) and best fit (solid lines) based on reaction Scheme 1 (see the text) for a solution of 44BPY (10^{-2} M) and DABCO (1.6 M) in H_2O excited at 266 nm. The dashed lines correspond to the 365 and 381 nm kinetics calculated in the assumption of an exclusive T_1 state origin of the anion radical. Inset a shows an enlargement of the early time (0−200 ps) kinetics. Inset b shows early time (0−200 ps) detail of the 381 nm kinetics and decomposition of the calculated fit (full line) into the individual contributions of the S_1 state and anion radical species (dotted lines).

SCHEME 1

$$S_1 \xrightarrow[k_{ISC}]{} T_1$$

$$S_1 \xrightarrow[k_q^1]{\text{DABCO}} \begin{cases} R^{-\cdot} & (\Phi_{et}^1) \\ S_0 & (\Phi_{deac}^1) \end{cases}$$

$$(S_1, \text{DABCO}) \xrightarrow[k_{st}^1]{} \begin{cases} R^{-\cdot} & (\Phi_{et}^1) \\ S_0 & (\Phi_{deac}^1) \end{cases}$$

$$T_1 \xrightarrow[k_q^3]{\text{DABCO}} R^{-\cdot} \quad (\Phi_{et}^3)$$

$$R^{-\cdot} \xrightarrow[k_H]{H_2O} RH^{\cdot}$$

In contrast, a biexponential decay kinetics is found for the S_1 state. A first decay component is characterized by a rate constant k_a^1 linearly increasing with the DABCO concentration. It corresponds thus to diffusional electron-transfer quenching: $k_a^1 = k_{ISC} + k_q^1$[DABCO] with $k_{ISC} = (2.8 \pm 0.1) \times 10^{10}$ s^{-1} (see part A) and a quenching rate constant $k_q^1 = (1.7 \pm 0.5) \times 10^{10}$ M^{-1} s^{-1}. A second, faster component is observed at high DABCO concentration. Its contribution in the S_1 state decay kinetics becomes significant for [DABCO] ≥ 1 M. Its rate

constant, k_b^1, is roughly independent of the DABCO concentration ($1/k_b^1 = 3 \pm 1$ ps). This fast kinetics indicates that part of the 44BPY S_1 state population is concerned with static electron-transfer quenching, that is, electron transfer from a DABCO molecule in close contact: $k_b^1 = k_{ISC} + k_{st}^1$ (k_{st}^1 = static quenching rate constant). In fact, at high amine concentration, the distribution of amines about 44BPY is such that a significant fraction of the 44BPY molecules should have an amine within the first solvent shell (population noted (S_0, DABCO) in Scheme 1). Similar processes of electron-transfer static quenching within the first solvent shell have been observed to occur in less than 20 ps in the photoreduction of benzophenone[19] and anthracene[20] derivatives (static quenching is different from the direct electron-transfer process occurring on excitation of ground-state charge-transfer complexes. In the case of the 44BPY/DABCO system, we found no indication of the existence of such a ground-state complex). In reality, intersystem crossing ($1/k_{ISC} = 36$ ps) cannot compete with static electron transfer, so $k_b^1 \cong k_{st}^1$. The appearance kinetics of the T_1 state, well-fitted by a single-exponential growth of rate constant k_a^1, is in agreement with this observation. Moreover, at 1.6 M DABCO (Figure 6) at which the contributions of the S_1 state static and diffusional quenching processes are found to be 32% and 68%, respectively, the amplitude of the T_1 kinetics is indeed in agreement with an intersystem crossing process originating from only two-thirds of the initial S_1 population.

Comparing Figures 1 and 2 reveals that the quenching of the S_1 state by DABCO ($k_q^1 + k_{st}^1$) reduces considerably the T_1 state yield but does not lead to important amounts of the photoreduction products. The absorption bands due to the anion radical and N-hydro radical species are dramatically weak at the end of the S_1 state decay (60 ps spectrum in Figure 2) and are growing essentially during the T_1 state decay in the 60−700 ps time range (Figure 3). The quenching reaction involving the S_1 state appears to be thus strongly unproductive, and a quenching-induced deactivation pathway with quantum yield $\Phi_{deac}^1 = 1 - \Phi_{et}^1$ was incorporated in the kinetic model (Scheme 1) to account for this observation. In contrast, the yield Φ_{et}^3 of formation of the anion radical from quenching of the T_1 state was nearly unity. Assuming that the anion radical originates exclusively from the T_1 state ($\Phi_{deac}^1 = 1$) leads to the simulated kinetic plots indicated by dashed lines in Figure 6. Obviously, the predicted rise of the anion radical is too slow at short times, which leads to an underestimated S_1 + anion kinetic plot in the 10−150 ps time domain (inset a in Figure 6). Also the kinetics calculated in this case for the N-hydro radical lies below the experimental data at all times. The best fit (full lines in Figure 6) is obtained for a deactivation yield of $\Phi_{deac}^1 = 0.95 \pm 0.02$, which means that only 5% of the excited S_1 molecules that are quenched by DABCO lead effectively to the production of the anion radical. Finally, the anion radical decay and the N-hydro radical growth were well-fitted by a single-exponential kinetics, which denotes a first-order or pseudo-first-order proton-transfer process. The corresponding rate constant, k_H, was found to decrease with increasing DABCO concentration on the 0.5 M ($1/k_H = 13$ ps) to 1.6 M ($1/k_H = 40$ ps) range. The anion species is produced as long as the triplet state is present. This explains why, despite its short lifetime, it is observed as a "stationary" intermediate on a 60−700 ps time range with an apparent decay kinetics following the T_1 state decay kinetics (see Figure 6).

The relative amplitudes of the kinetic curves calculated for the S_1 state, the T_1 state, the anion radical, and the N-hydro radical were set on the basis of a 1:1.5:0.9:1 ratio of the respective extinction coefficients in water solvent and adjusted to the experimental data according to the initial S_1 state absorption. The relative S_1 and T_1 coefficients were estimated from the ratio of the T_1 band intensity at the end of the $S_1 \rightarrow T_1$ kinetics and initial S_1 band intensity obtained by extrapolating the exponential decay fit of the S_1 absorption at time zero in water in the absence of DABCO (Figure 1). The relative anion radical extinction coefficient was that previously deduced from the initial T_1 absorption and final anion absorption in the case of photoreduction by DABCO in acetonitrile.[13] Finally, the relative N-hydro radical coefficient was deduced similarly from the initial T_1 state absorption in the reaction of photoabstraction of hydrogen atom from 2-propanol.[5] We observe in Figure 6 that there is a good agreement between the experimental and calculated kinetics concerning the profiles, as well as the relative amplitudes. The main rate constant values are summarized in Table 1. Fits of comparable quality were obtained for the different DABCO concentrations (0.5−1.6 M range) experienced in this investigation.

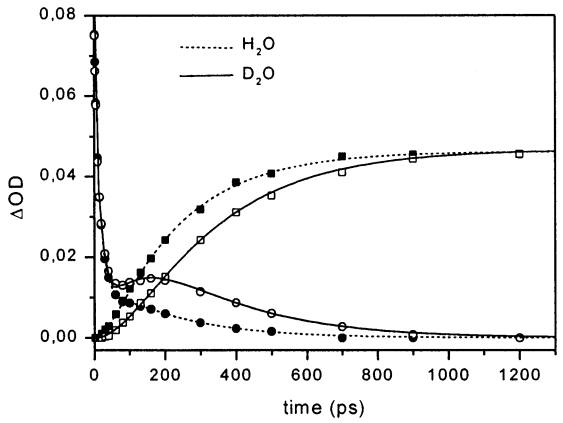

Figure 7. Time dependence of the extracted contribution of the N-hydro radical absorption at 365 nm (□) and of the residual absorption (S_1 state + anion radical) at 381 nm (○) and best fit (solid lines) based on reaction Scheme 1 (see the text) for a solution of 44BPY (10^{-2} M) and DABCO (1.6 M) in D_2O excited at 266 nm. The corresponding data (■ and ●, respectively) and calculated fits (dashed lines) obtained in H_2O are also given for comparison.

TABLE 1: Summary of the Kinetic Parameters Involved in the Photoreduction of 44BPY by DABCO in H_2O, D_2O, and H_2O + KOH (1 M) Solutions (Scheme 2)

	H_2O	D_2O	H_2O + KOH (1 M)
k_{ISC} (10^{10} s^{-1})	2.8 ± 0.1	2.8 ± 0.1	3.1 ± 0.1
k_q^1 (10^{10} M^{-1} s^{-1})	1.7 ± 0.5	1.5 ± 0.5	1.8 ± 0.5
k_{st}^1 (10^{10} s^{-1})	33 ± 11	31 ± 10	33 ± 11
k_q^3 (10^{10} M^{-1} s^{-1})	0.48 ± 0.03	0.40 ± 0.03	0.44 ± 0.03
$k_{H(D)}$ (10^{10} s^{-1}), 0.5 M DABCO	7.7 ± 2.0	3.0 ± 1.0	2.5 ± 1.0
$k_{H(D)}$ (10^{10} s^{-1}), 1.6 M DABCO	2.5 ± 1.0	1.0 ± 0.5	2.0 ± 1.0
Φ_{deac}^1	0.95 ± 0.02	0.94 ± 0.02	0.94 ± 0.02
Φ_{et}^1	0.05 ± 0.02	0.06 ± 0.02	0.06 ± 0.02
Φ_{et}^3	~1	~1	~1

C. Kinetic Isotope Effect in D_2O. Changing the solvent from H_2O to D_2O was found to modify the reaction kinetics. Figure 7 shows the time evolution of the S_1 state + anion radical contribution to the absorption at 381 nm on one hand (circle symbols) and of the N-hydro radical absorption contribution at 365 nm on the other hand (square symbols) in the case of photoreduction of 44BPY by DABCO (1.6 M) in D_2O (open symbols). The corresponding data obtained in H_2O (taken from Figure 6) are displayed in the figure for comparison (solid

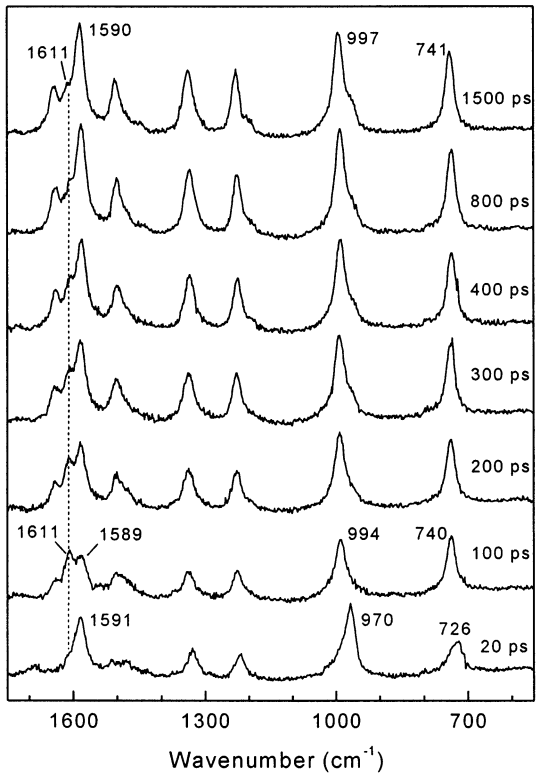

Figure 8. Time-resolved resonance Raman spectra of a solution of 44BPY (10^{-3} M), DABCO (1 M), and KOH (1M) in H_2O probed at 380 nm at different delay times (20−1500 ps) after pump excitation at 253 nm. The probe-only spectrum (solvent and ground-state peaks) has been subtracted to all spectra. Some characteristic Raman frequencies are indicated. The dashed line points out the position of the 1611 cm^{-1} band typical of the anion radical $44BPY^{-\bullet}$.

symbols). Also shown in the figure are the theoretical fits obtained by using the above reaction model with the rate constant values given in Table 1. The major change observed on going from H_2O to D_2O solvent is a significant slowing of the anion radical decay and N-hydro radical rise kinetics, which is indicative of a slower rate constant for deuteron transfer (k_D) than for proton transfer (k_H). The measured kinetic isotope effect is $k_H/k_D = 2.5$. A small reduction of the quenching rate constants k_q^1 and k_q^3 is also remarked in D_2O.

D. Influence of KOH. To analyze the influence of pH on the kinetics of protonation of the bipyridine anion radical, the photoreduction of 44BPY by DABCO has also been investigated in aqueous solutions containing 1 M KOH. Measurements were made for two DABCO concentrations, 0.5 and 1.6 M. In both cases, the evolution of the transient absorption spectra is essentially similar to that observed in Figures 2 and 3 in the absence of KOH. However, at long time delays (>500 ps), the UV and visible absorption bands of the N-hydro radical species show a slightly broader band foot on the low-energy side, that is, at the position of the absorption bands of the anion radical. As a matter of fact, subtracting the 1.5 ns spectrum obtained in the absence of KOH from that obtained with 1 M KOH leads to a spectrum comparable in band shape and position to the anion radical spectrum observed in the absence of KOH. This observation is confirmed by the time-resolved resonance Raman measurements displayed in Figure 8: the spectra probed at 380 nm, in optimum resonance with the anion radical absorption, clearly show that the 1611 cm^{-1} Raman peak characteristic of the anion radical (indicated with a dashed line in the figure) survives at 1500 ps. The residual anion spectrum obtained by subtracting the N-hydro radical contribution at 1500 ps is

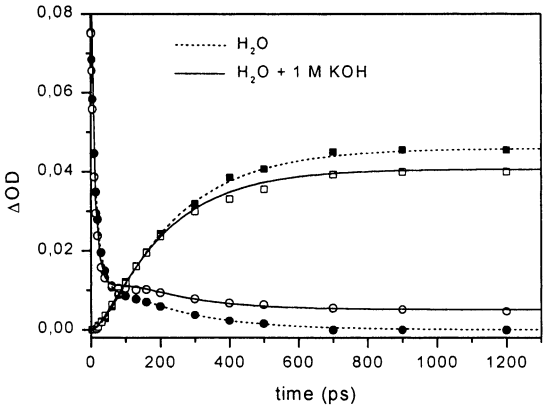

Figure 9. Time dependence of the extracted contribution of the N-hydro radical absorption at 365 nm (□) and of the residual absorption (S_1 state + anion radical) at 381 nm (○) and best fit (solid lines) based on reaction Scheme 1 (see the text) for a solution of 44BPY (10^{-2} M), DABCO (1.6 M), and KOH (1 M) in H_2O excited at 266 nm. The corresponding data (■ and ●, respectively) and calculated fits (dashed lines) obtained in the absence of KOH are also given for comparison.

characterized by the same band frequencies as those found at 100 ps in the absence of KOH (bottom spectrum in Figure 5). The kinetic data obtained from the absorption measurements in the case of 1.6 M DABCO concentration are shown in Figure 9 for the S_1 state + anion radical contribution at 381 nm and the N-hydro radical contribution at 365 nm (open symbols). The data obtained in the absence of KOH (taken from Figure 6) are also shown for comparison (solid symbols). These data confirm clearly that the anion radical does not disappear completely when KOH is present. The anion radical and N-hydro radical populations appear to be stabilized after 600 ps. The best theoretical fits are also displayed in Figure 9. The rate constants corresponding to these fits are listed in Table 1. The reaction model used for the fit is the same as that established above (Scheme 1), but it has been modified to incorporate an acid−base equilibrium between the anion and N-hydro radicals. The relative amounts of the two species at equilibrium are found to be 9% ± 2% and 91% ± 2%, respectively. These proportions are independent of the DABCO concentration, as expected from the fact that a constant pH of ca. 14 is imposed by the 1 M KOH content (the presence of DABCO does not modify significantly the basicity of the solution). An approximate pK_a value of 15 is thus deduced for the $44BPY^{-\bullet}$ species. This value is consistent with the lower limit of $pK_a > 14$ previously reported for this anion.[14]

4. Discussion

The reaction model of Scheme 1 allows reproducing of all of the kinetic data observed for the photoreduction of 44BPY by DABCO in H_2O, H_2O + 1 M KOH, and D_2O solutions for different amounts of the DABCO quencher. For each experiment, both the profiles and relative amplitudes of the S_1 state, T_1 state, anion radical, and N-hydro radical kinetics are properly fitted. This correlation confirms the sequential electron-transfer−proton-transfer mechanism.

The S_1 state reaction is nearly unproductive ($\Phi_{et}^1 = 0.05$), although strong excited singlet-state quenching is observed ($k_q^1 = 1.7 \times 10^{10}\ M^{-1}\ s^{-1}$). The same situation was previously found in acetonitrile solvent,[13] in which case it was concluded on the basis of thermodynamical considerations that the low yield of anion radical was the result of an ultrafast, spin-allowed back electron transfer occurring within the singlet ion pair formed initially from the forward electron-transfer process. It is reason-

able to assume that, in the case of water solvent, intrapair back electron-transfer deactivation process also competes with the dissociation of the pair into free ions. In this hypothesis, the dissociation to deactivation yield ratio measured in aqueous solution, $\Phi^1_{et}/\Phi^1_{deac} = 0.05{:}0.95$, implies that the intrapair charge recombination is ~20 times faster than the dissociation of the pair. The singlet ion pair considered in this analysis is supposed to result indistinguishably from the two types of electron-transfer quenching processes, static and diffusional, identified in the above kinetic analysis. In reality, different ion pairs with specific structures and deactivation to dissociation yield ratios may be formed in these two reactions. Differentiating these specific behaviors should be possible in principle from transient absorption by analyzing the short-time kinetics of the anion radical. However, because of the extremely low amount of anion issuing from the S_1 state and also the close resemblance of the anion and S_1 spectra, distinguishing two components in the short-time anion kinetics was unfeasible.

The diffusional quenching rate constants k^1_q and k^3_q observed for the photoreduction of 44BPY by DABCO in water (1.7×10^{10} and 4.8×10^9 M^{-1} s^{-1}, respectively) are weaker than those found previously[13] in acetonitrile (3.5×10^{10} and 1.2×10^{10} M^{-1} s^{-1}, respectively). The corresponding drops by factors 2.06 (k^1_q) and 2.5 (k^3_q) are consistent with the increase in the solvent viscosity in going from acetonitrile to water ($\eta_{water}/\eta_{acetonitrile} = 2.6$) and can thus be accounted for by changes in the rate constant of diffusion in the two solvents. Similarly, the reduction of the electron-transfer rate constant by factors of 1.13 (k^1_q) and 1.2 (k^3_q) in going from H_2O to D_2O (see Table 1) correlates approximately to the increase in viscosity of H_2O compared to D_2O ($\eta_{H_2O}/\eta_{D_2O} = 1.25$). Another effect that might contribute to the observed decrease in the electron-transfer rates in water compared to acetonitrile is the fact that, as shown above, the ground-state bipyridine and amine species are hydrogen-bonded in aqueous solution. In fact hydrogen bonding with DABCO is expected to increase the activation energy for the reaction because the hydrogen bond must be broken prior to transfer.[21]

As discussed above, the existence of a singlet ion pair is deduced indirectly from the observation of an ultrafast, non-diffusional back electron-transfer process. In the case of the triplet state quenching reaction, there is no kinetic manifestation of a triplet ion pair because no specific intrapair reaction takes place. From a spectroscopic point of view, no change in band shape and position is perceptible in the UV−visible absorption spectrum of the 44BPY anion radical during the 0−700 ps time range when this species is present. This spectrum is also identical to the residual anion spectrum observed in the presence of 1 M KOH at 1500 ps. This is consistent with our previous report that in acetonitrile, in which a contact ion pair is formed upon photoreduction, the free and ion-paired $44BPY^{-\bullet}$ have identical absorption spectra.[13] However, also in this study, it was found that the free and ion-paired anion species are distinguishable from Raman spectroscopy by slightly different vibrational frequencies in such a way that, in acetonitrile, a progressive shift of the band frequencies with time characterized the dissociation of the ion pair into the free ions.[13] This shift reflects the high sensitivity of some vibrational modes of $44BPY^{-\bullet}$ to the changes of the ion environment accompanying the ion pair dissociation. These changes can be of two types: an increase of the ion solvation and the cancellation of the intrapair electronic coupling. In contrast, we observe here that, in water, the $44BPY^{-\bullet}$ Raman bands do not manifest any significant frequency shift with time (Figures 4 and 8). Before discussing the different behavior observed in acetonitrile and in water, it is worth remarking that the three Raman peaks of the anion species lying at 1611, 1509, and 992 cm^{-1} in water (bottom trace in Figure 5) have notably higher frequencies than those previously measured for the free anion in acetonitrile[13] ($\Delta\nu = +5$, +8, and +9 cm^{-1}, respectively). A fourth line at 741 cm^{-1} shows a less significant shift ($\Delta\nu = +3$ cm^{-1}). According to the assignment of the anion radical vibrations established on the basis of ab initio calculations,[10] these lines correspond to the ring distortion modes 8a, 19a, 12, and 1. These are precisely the modes that have been underlined as sensitive to H-bonding in the case of the ground-state molecule ($\Delta\nu = +7$, +7, +11, and +8 cm^{-1}, respectively; see the Results section) and of the N-hydro radical ($\Delta\nu = +12$, +9, +10, and +4 cm^{-1}, respectively).[7] We ascribe thus the mode-specific frequency shifts observed in the anion radical Raman spectrum on going from acetonitrile to water solvent to the presence of hydrogen bonds in the latter case. On the other hand, the absence of any time dependence of the frequency values in water, even at the shortest time delays, indicates that the anion radical is H-bonded as soon as it is produced.

On the basis of these results, an open question concerns the nature of the ion pair formed in these conditions: does the occurrence of H-bonding between water and the ground-state parent molecules, 44BPY and DABCO, and also the reduction product, $44BPY^{-\bullet}$, imply that the ion pair produced in water differs in nature from the contact ion pair (CIP) formed in acetonitrile? Considering that the electron-donor center of DABCO is restricted to the N-atoms, steric hindrance by H-bonding is expected to prevent any close contact between the donor center and the acceptor molecule. This point and the fact that the $44BPY^{-\bullet}$ anion radical is also H-bonded as soon as it is produced suggest that the electron transfer could occur through a solvent layer and lead to the formation of a solvent-separated ion pair (SSIP). In this respect, the fact that the dissociation of the ion pair into free ions has been characterized by significant frequency shifts in the Raman spectrum of $44BPY^{-\bullet}$ in acetonitrile but not in water could be explained by the different state of solvation of the ions in the two types of pairs. As discussed by Gould et al.,[22] the overall solvation of the ions is weaker in a CIP compared to that in a SSIP. This results from the fact that, first, there are no solvent molecules between the ions in a CIP. Second, the two ions being closer together in a CIP than in a SSIP, their opposite orienting influences on the solvent shell cancel each other out notably more in the case of CIP. As a consequence, a larger change in solvation is expected on going to the free ions from a CIP than from a SSIP. A larger change in electronic coupling is expected as well. Thus the environment of the ions is presumed to be so similar in a SSIP and in the bulk solution that the dissociation of the SSIP could arise without any perceptible change of the vibrational frequencies. However, it is worth remarking that the absence of perceptible frequency shifts with time in the $44BPY^{-\bullet}$ Raman spectrum recorded in water may have other causes than a change in the ion pair nature. It could result from a lower sensitivity to the environment of the $44BPY^{-\bullet}$ normal modes in water than that in acetonitrile due to H-bonding. It could also result from slower ion pair dissociation in water because of its high viscosity compared to acetonitrile. In fact, in this hypothesis, the $44BPY^{-\bullet}$ ion may decay by proton transfer from water while still in the pair. Thus, the suggestion that a SSIP is formed upon photoreduction of 44BPY in water remains tentative at the moment.

As observed for the Raman spectrum, the transient absorption spectrum in water differs from that in acetonitrile. A notable

SCHEME 2

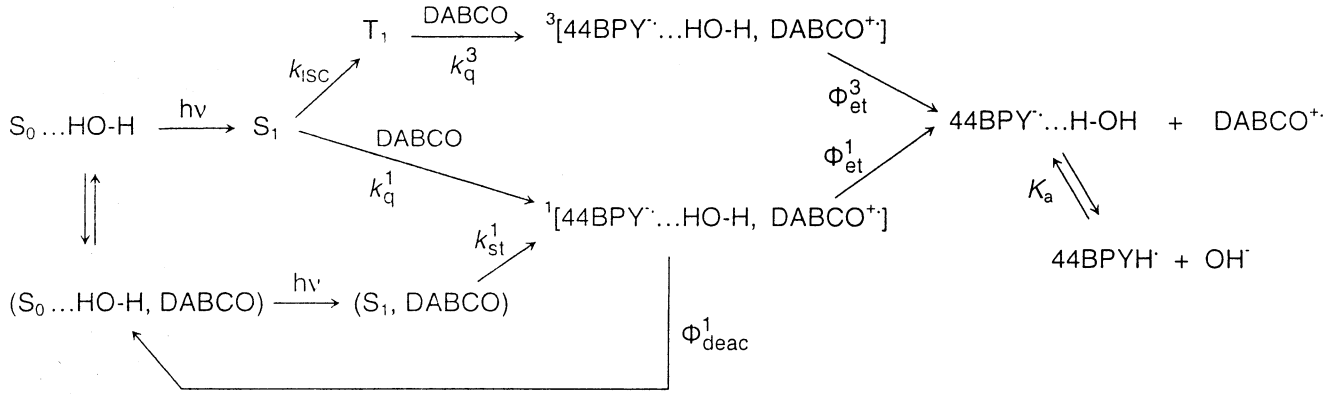

shift to higher energy characterizes the visible band (vibronic maxima at 555, 580, and 638 nm in acetonitrile and at 530, 562, and 604 nm in water), whereas the position of the UV band remains unchanged (maximum at 379 ± 1 nm). According to the above discussion of the Raman data, this shift effect can be ascribed to the presence of H-bonding in water. On the basis of semiempirical[6] and ab initio[23] calculations, the visible absorption of $44BPY^{-\bullet}$ has been ascribed to a quasi-one-electron $\pi\pi^*$ transition involving the unpaired electron derived from the $\Phi_7 \rightarrow \Phi_{10}$ excitation of the biphenyl anion radical.[24,25] As a matter of fact, a manifest resemblance noticed between the UV−visible absorption and resonance Raman spectra of $44BPY^{-\bullet}$, on one hand, and those reported[24−28] for the biphenyl anion radical, on the other hand, provided an experimental confirmation of the analogous electronic properties of these two ions.[4,6] According to the structure and electronic configuration of $44BPY^{-\bullet}$,[10,11] the negative charge is essentially localized on the nitrogen atoms. H-bonding is thus expected to stabilize this configuration in such a way that a higher energy must be required to excite the unpaired electron in protic solvents than in aprotic solvents. This is consistent with the increase in energy observed for the absorption band associated with the $\Phi_7 \rightarrow \Phi_{10}$ excitation in going from acetonitrile to water. However, rigorously, this assumption is correct only if the electronic configuration of the upper state involved in the transition is less-stabilized by H-bonding than the ground state, that is, if the charge is more delocalized on the rings after excitation. Therefore, the $\pi\pi^*$ $\Phi_7 \rightarrow \Phi_{10}$ transition of the $44BPY^{-\bullet}$ species contains probably some character of charge transfer from the nitrogen atom to the ring.

Finally, the presence of H-bonding between $44BPY^{-\bullet}$ and water implies that the protonation of the anion radical by water to yield the N-hydro radical occurs through the hydrogen bond. Therefore, at first sight, this process might be considered as a nondiffusional, intracomplex reaction, in agreement with the observed first-order kinetics. In this perspective, according to recent theoretical developments relating to proton transfer in solution phase,[29−31] the small kinetic isotope effect (k_H/k_D = 2.5) suggests that the proton-transfer process is adiabatic, that is, it does not occur via proton tunneling. Adiabatic proton transfer is expected along strong hydrogen bonds, in which case the small intrinsic barrier allows large proton coupling. However, with respect to the fact that the ($44BPY^{-\bullet}\cdots H_2O$) complex is not isolated in the solvent but is linked to the surrounding water molecules through an extended hydrogen-bond network, the reaction is probably more complex than a simple intracomplex transfer and may involve collective molecular motions associated with the rearrangement of the hydrogen-bond network. The observation that the proton-transfer rate constant, k_H, decreases with increasing DABCO concentration emphasizes the role played by the environment in the reaction dynamics. From evidence, the basic poles represented by the amine molecules disseminated in the solution exert a significant long-distance influence, through the hydrogen-bond network, on the dynamics of intracomplex proton jump. In this regard, the effect of increasing the DABCO concentration on k_H may result from a reduction of the proton-donor ability of the water molecule bonded to the ion (decrease of local acidity), a lengthening of the N···H distance between the $44BPY^{-\bullet}$ acceptor and water donor in the H-bonded complex (structural change of the water network), or a reduction of the ability of the solution to accommodate the OH^- species produced after proton transfer (solvation effect). The results obtained at pH 14 (1 M KOH) show that the reaction leads to a mixture of the neutral ($44BPYH^{\bullet}$) and ionic ($44BPY^{-\bullet}$) species according to an acid−base equilibrium with $pK_a \cong 15$. This high pK_a value explains why, in the absence of KOH, the reaction is completely displaced toward the neutral radical form. In fact, at pH values of 11−12 (aqueous solution containing 0.1−1.6 M DABCO), a concentration ratio, $[44BPY^{-\bullet}]/[44BPYH^{\bullet}]$, of $10^{-3}-10^{-4}$ is expected at equilibrium, in which case the anion radical contribution in the spectra is too weak to be perceptible. As can be seen in Table 1, adding 1 M KOH to the 0.5 M DABCO solution reduces the protonation rate k_H in a similar way as increasing the DABCO concentration from 0.5 to 1.6 M. However, adding KOH to the 1.6 M DABCO solution does not affect notably the k_H value. The effect of pH on the rate of proton transfer k_H and on the acid−base equilibrium dynamics is thus not clear.

This reaction of fast protonation of the 44BPY anion radical can be related to the similar but opposite reaction of excited-state proton dissociation observed, for instance, for aromatic alcohols, ROH.[32,33] In fact, whereas the $44BPY^{-\bullet}$ species is more basic than the neutral parent molecule, aromatic alcohols are more acidic in their S_1 state than in S_0. Therefore, in both cases, the sudden introduction of a base/acid into an otherwise unchanged solution by photoexcitation gives rise to a pH jump and initiates a proton-transfer process from/to the solvent, leading to a release of OH^-/H^+ in the solution. The solvent molecule plays a dual role as OH^-/H^+ acceptor and as a solvating medium. In the case of excited-state proton transfer, a number of time-resolved investigations in different environments, for example, small molecular clusters[34,35] and solutions in water and in mixed water/organic solvents,[36−42] have evidenced the influence of water structure in the reaction kinetics, but the exact nature of the process remains not completely clear. The formation of water clusters as proton-solvating entities has been suggested to control the reaction

dynamics,[36,37] but this point is still debated. To get the same type of information about the role of water structure on the dynamics of proton abstraction by the 44BPY anion radical and understand the factors governing the dynamics of proton transfer along hydrogen bonds in aqueous solution, we are currently performing a systematic kinetic analysis of the photoreduction of 44BPY by aliphatic amines as a function of the pH in water and in a series of binary acetonitrile/water solutions.

5. Conclusion

In conclusion, the photoreduction of 44BPY by DABCO has been studied in water by picosecond transient absorption spectroscopy and time-resolved resonance Raman spectroscopy. The kinetics of formation of the anion radical $44BPY^{-\bullet}$ by electron transfer have been analyzed and compared with those obtained previously for the same reaction in acetonitrile. The overall mechanism is summarized in the reaction Scheme 2. It must be recalled that the term ($S_0\cdots HO-H$, DABCO) in Scheme 2 does not refer to a ground-state charge-transfer complex between 44BPY and DABCO but to the population of 44BPY molecules that have a DABCO species in the first solvent shell at the moment of the excitation. The whole set of kinetic parameters is reported in Table 1. The following results have been obtained:

(1) The rates of diffusional quenching of both the S_1 and T_1 states by electron transfer are lowered in going from acetonitrile to water solvent according to the increase of the medium viscosity.

(2) In water as in acetonitrile, the S_1 state reaction is essentially unproductive because of ultrafast intrapair back electron transfer. The anion radical $44BPY^{-\bullet}$ is essentially produced from the T_1 state.

(3) The $44BPY^{-\bullet}$ anion is linked by H-bonding to the surrounding water molecules immediately after its formation and undergoes proton transfer along the H-bond to reach an acid−base equilibrium of $pK_a \cong 15$ with the N-hydro radical $44BPYH^{\bullet}$. The precursor ground-state 44BPY and DABCO molecules are also H-bonded in aqueous solution prior to excitation.

(4) Whereas in acetonitrile a contact ion pair formed upon reduction could be distinguished from the free ions by the observation of specific Raman frequencies of the $44BPY^{-\bullet}$ anion, no such discrimination was possible in water. We suggest that, in aqueous solution, steric hindrance by H-bonding prevents any close contact between the acceptor and donor species. As a consequence, the reaction leads to the formation of a solvent-separated ion pair in which the environment of the ions is close to that in bulk water. However, we cannot rule out the possibility that quenching of the $44BPY^{-\bullet}$ anion by proton transfer from water arises within the ion pair before its dissociation, in which case no vibrational shifts are expected even if a contact ion pair is produced by electron transfer. More information on this point and on the dynamics of the proton transfer process should be obtained from similar time-resolved investigations of the 44BPY photoreduction reaction in mixed water/acetonitrile solutions. These experiments, currently in progress, will be the object of a further report.

Acknowledgment. The authors thank the Groupement de Recherche GDR 1017 from CNRS and the Centre d'études et de Recherches Lasers et Applications (CERLA) for their help in the development of this work. CERLA is supported by the Ministère chargé de la Recherche, Région Nord/Pas de Calais, and the Fonds Européen de Développement Economique des Régions.

References and Notes

(1) Buntinx, G.; Naskrecki, R.; Poizat, O. *J. Phys. Chem.* **1996**, *100*, 19380.
(2) Didierjean, C.; Buntinx, G.; Poizat, O. *J. Phys. Chem. A* **1998**, *102*, 7938.
(3) Didierjean, C.; Dewaele, V.; Buntinx, G.; Poizat, O. *Chem. Phys.* **1998**, *237*, 169.
(4) Buntinx, G.; Valat, P.; Wintgens, V.; Poizat, O. *J. Phys. Chem.* **1991**, *95*, 9347.
(5) Poizat, O.; Buntinx, G.; Valat, P.; Wintgens, V.; Bridoux, M. *J. Phys. Chem.* **1993**, *97*, 5905.
(6) Kihara, H.; Gondo, Y. *J. Raman Spectrosc.* **1986**, *17*, 263.
(7) Poizat, O.; Buntinx, G.; Ventura, M.; Lautié, M. F. *J. Phys. Chem.* **1991**, *95*, 1245.
(8) Simic, M.; Ebert, M. *Int. J. Radiat. Phys. Chem.* **1971**, *3*, 259.
(9) Elisei, F.; Mazzucato, U.; Görner, H.; Schulte-Frohlinde, D. *J. Photochem. Photobiol. A* **1989**, *50*, 209.
(10) Ould-Moussa, L.; Poizat, O.; Castella-Ventura, M.; Buntinx, G.; Kassab, E. *J. Phys. Chem.* **1996**, *100*, 2072.
(11) Castella-Ventura, M.; Kassab, E. *J. Raman Spectrosc.* **1998**, *29*, 511.
(12) Dewaele, V.; Buntinx, G.; Poizat, O.; Flament, J.-P.; Kassab, E. *J. Chem. Phys.* **1999**, *110*, 6353.
(13) Boilet, L.; Burdzinski, G.; Buntinx, G.; Lefumeux, C.; Poizat, O. *J. Phys. Chem. A* **2001**, *105*, 10271.
(14) Fessenden, R. W.; Neta, P. *Chem. Phys. Lett.* **1973**, *18*, 14.
(15) Cohen, G.; Parola, A.; Parsons, G. H. *Chem. Rev.* **1973**, *73*, 141.
(16) Devadoss, C.; Fessenden, R. W. *J. Phys. Chem.* **1991**, *95*, 7253.
(17) Paoletti, P.; Stern, J. H.; Vacca, A. *J. Phys. Chem.* **1965**, *69*, 3759.
(18) Balakrishnan, G.; Keszthelyi, T.; Wilbrandt, R.; Zwier, J. M.; Brouwer, A. M.; Buma, W. J. *J. Phys. Chem. A* **2000**, *104*, 1834.
(19) Peters, K. S.; Lee, J. *J. Phys. Chem.* **1993**, *97*, 3761.
(20) Vauthey, E. *J. Phys. Chem. A* **2001**, *105*, 340.
(21) Simon, J. D.; Peters, K. S. *J. Am. Chem. Soc.* **1982**, *104*, 6542.
(22) Gould, I. R.; Young, R. H.; Moody, R. E.; Farid, S. *J. Phys. Chem.* **1991**, *95*, 2068.
(23) Lapouge, C.; Buntinx, G.; Poizat, O. *J. Phys. Chem. A* **2002**, *106*, 4168.
(24) Zahradnik, R.; Carsky, P. *J. Phys. Chem.* **1970**, *74*, 1240.
(25) Matsunuma, S.; Yamaguchi, S.; Hirose, C.; Maeda, S. *J. Phys. Chem.* **1988**, *92*, 1777.
(26) Shida, T.; Iwata, S. *J. Am. Chem. Soc.* **1973**, *95*, 3473.
(27) Yamaguchi, S.; Yoshimizu, N.; Maeda, S. *J. Phys. Chem.* **1978**, *82*, 1078.
(28) Aleksandrov, V.; Bobovitch, Y. G.; Maslov, V. G.; Sidirov, A. N. *Opt. Spectrosc.* **1975**, *38*, 387.
(29) Borgis, D. C.; Lee, S.; Hynes, J. T. *Chem. Phys. Lett.* **1989**, *162*, 19.
(30) Borgis, D. C.; Hynes, J. T. *J. Chem. Phys.* **1991**, *94*, 3619.
(31) Borgis, D. C.; Hynes, J. T. *J. Phys. Chem.* **1996**, *100*, 1118.
(32) Weller, A. *Prog. React. Kinet.* **1961**, *1*, 187.
(33) Kosower, E. M.; Huppert, D. *Annu. Rev. Chem.* **1986**, *37*, 127.
(34) Syage, J. A. *J. Phys. Chem.* **1995**, *99*, 5772.
(35) Zhong, Q.; Castleman, A. V., Jr. *Chem. Rev.* **2000**, *100*, 4039.
(36) Fillingim, T. G.; Luo, N.; Lee, J.; Robinson, G. W. *J. Phys. Chem.* **1990**, *94*, 6368.
(37) Robinson, G. W. *J. Phys. Chem.* **1991**, *95*, 10386.
(38) Agmon, N.; Huppert, D.; Masad, A.; Pines, E. *J. Phys. Chem.* **1991**, *95*, 10407.
(39) Pines, E.; Fleming, G. R. *J. Phys. Chem.* **1991**, *95*, 10448.
(40) Solntsev, K. M.; Huppert, D.; Agmon, N. *J. Phys. Chem. A* **1999**, *103*, 6984.
(41) Solntsev, K. M.; Huppert, D.; Agmon, N.; Tolbert, L. M. *J. Phys. Chem. A* **2000**, *104*, 4658.
(42) Tolbert, L. M.; Solntsev, K. M. *Acc. Chem. Res.* **2002**, *35*, 19.